BŞEÜ Fen Bilimleri Dergisi
6 (1), 12-23, 2019

BSEU Journal of Science
DOI: 10.35193/bseufbd.554791

e-ISSN: 2458-7575 (http://dergipark.gov.tr/bseufbd)

Araştırma Makalesi – Research Article

A Novel Stress-Level-Specific Feature Ensemble for Drivers' Stress Level Recognition

İdil IŞIKLI ESENER[1*]

Geliş / Received: 17/04/2019 ***Revize / Revised: 01/05/2019*** ***Kabul / Accepted: 03/05/2019***

Abstract- **This paper proposes a novel feature set for drivers' stress level recognition. The proposed feature set consists of data-independent and almost uncorrelated feature pairs for each stress level with very strong intra-class and relatively weak inter-class correlations, constructed by realizing a correlation analysis on the popular features studied in the literature. By using the proposed feature set, a maximum of 100% stress level recognition accuracy is achieved with an average increment of 24.85% while a mean reduction rate of 88.01% is satisfied in false positive rate compared to the full feature set. These outcomes clearly show that the proposed feature set can confidently be integrated into the driving assistance systems.**

***Keywords*- Stress Recognition, Feature Selection, Feature Correlation**

I. INTRODUCTION

Distress (negative stress), the negative emotions and unexpected behaviors of an individual as a result of physical and emotional deterioration, is analyzed as acute, episodic acute and chronic stress due to its effects and duration of these effects [1, 2]. It is known that the effects of distress on drivers affect the driving performance negatively, concluding in traffic violations or accidents [3, 4]. Related studies show that the drivers mostly experience acute stress due to road conditions, traffic density, social interactions, unexpected situations, other drivers' or pedestrians' behaviors, events that impact time schedule, and difficult driving due to urban planning [5, 6]. Acute stress is known to be a short-term stress caused by daily life stressors related to recent past or near future [5], and by stimulating the sympathetic nervous system, it physiologically shows itself in increments in blood sugar level, respiration rate, number of heartbeat, blood pressure, and muscle activity; shortness of breath, sweaty palms, cold hands or foots, dizziness, chest pain, headache, activation of the blood coagulation mechanism, irritable bowel syndrome and pupil dilation [7]. Electrocardiogram (ECG), Photoplethysmogram (PPG), Galvanic Skin Response (GSR), Electromyogram (EMG), and Respiration (RESP) are the physical sensors used for digitizing these effects.

In this paper, a correlation analysis of a number of popular measurements computed from the mentioned physical sensors with each other and also with the stress levels is made. As the result of this analysis, the full correlated measurements with each other are eliminated, and the very strongly correlated measurements with each stress level are determined. These measurements are then used for stress level recognition by using Logistic Linear Classifier (LLC), k-Nearest Neighbor (kNN), random forest, decision tree, and Support Vector Machines (SVM) classifiers. The accuracy in stress level recognition is reached up to 100%, and shows a remarkable amount of increment against when all of the measurements are utilized.

This paper is organized as follows: the studies related with stress level recognition in the literature are summarized in the following section. In Section 3, the experimental studies are explicitly defined and the succeeded results and discussions on these results are given in Section 4. The main conclusions are indicated in the last section.

[1]*Sorumlu yazar iletişim: idil.isikli@bilecik.edu.tr (https://orcid.org/0000-0002-0136-7635)
Department of Electrical and Electronics Engineering, Bilecik Şeyh Edebali Univ. Bilecik

II. BACKGROUND

The studies related to stress recognition analyze the stress responses on sympathetic nervous system and parasympathetic nervous system based on the fact that SNS is stimulated in a stressed state, and PNS in a relaxed state [2]. These analyses are widely realized on ECG [7-18, 20-27], GSR [7-14, 16, 17, 19, 20, 23, 25-27], RESP [7, 9-17, 20, 23, 25, 26], EMG [7, 9-11, 14, 16, 17, 20, 21, 26], and PPG [19] signals.

The variations in the heart beats are analyzed by Heart Rate (HR) and Heart Rate Variability (HRV) measurements using ECG [7-18, 20-27] and PPG [19] signals. Heart rate is the frequency of heart beats per minute, and HRV indicates the variations between heart beats. The most utilized measurements for HR are the mean (MHR) [7, 11, 14, 16, 17, 20, 22, 25-27] and the standard deviation (SDHR) [11, 14, 16, 17, 20, 25] of heart rate. The median of HR [20], variance of HR [20], maximum HR [27], and minimum HR [27] are also used for HR analyses.

The HRV is analyzed on both time and spectral domain. The time-domain measurements for HRV include the mean of N-to-N intervals (MNN) [19, 23], the standard deviation of N-to-N intervals (SDNN) [18, 19, 23, 24], the root-mean-square of successive interval differences (RMSSD) [18, 19, 23, 26], the triangular interpolation of the N-to-N interval histogram [23], the number of N-to-N interval differences differ by more than 50 milliseconds (NN50) [18], the percentage of NN50 over the number of heart beats (pNN50) [18, 19, 23], the percentage of the number of N-to-N interval differences differ by more than 20 milliseconds over the number of heart beats (pNN20) [19], the mean of first differences (MFD) [7,18, 22], the mean of second differences (MSD) [18], the mean of QRS-to-QRS intervals (MQRS) [22], the mean of R-to-R intervals (MRR) [22], the mean of Q-to-Q intervals (MQQ) [22], the mean of S-to-S intervals (MSS) [22], the mean of Q-to-R intervals (MQR) [22], the mean of R-to-S intervals (MRS) [22], the PPG pulse height [19], the PPG rise time [19], the PPG fall time [19], the PPG cardiac period [19], the PPG instantaneous heart rate [19], and the heart rate variation from baseline [8]. The total spectral power (TP) [19], the spectral powers of very low frequency band (VLF) [18, 19, 23], the low frequency band (LF) [9, 10, 14, 17-19, 23, 25, 26], the high frequency band (HF) [9, 10, 18, 19, 23, 25, 26], and the LF/HF ratio [9, 10, 12, 13, 18, 19, 23-26] are the frequently used HRV measurements in Fourier domain. Besides, the VLF/TP ratio [12, 13], the LF/VLF ratio [12, 13], the HF/VLF ratio [12, 13], the spectrum entropy [12]; the QRS power spectrum [15], the power samples of the R-peaks [21], the mean and the standard deviation in Wavelet domain [25] are also used for spectral HRV analysis.

Sweaty palms and cold hands or foots cause changes on skin conductance (SC) of human body. In the literature, the SC is analyzed in three groups. One of the group of features are directly extracted from the GSR and includes the mean (MSC) [9, 11, 14, 16, 17, 20, 25, 27], the median [20], the variance (VarSC) [9, 20], the standard deviation (SDSC) [11, 1, 17, 20, 25], the maximum [27] and the minimum [27] of the skin conductivity. Another group analyzes the Skin Conductance Level (SCL – the tonic component of GSR) by means of the mean of SCLs (MSCL) [23, 26] and the variance of SCLs (VarSCL) [23]. The most popular group analyzes the Skin Conductance Response (SCR – the phasic component of GSR) through the sum of frequency of occurrence [9], the number of peaks [19, 25, 27], the number of local maxima [26], the number of SCRs (NSCR) [10, 14, 17, 23], the rate of SCR (RSCR) [7], the mean of SCRs (MSCR) [7, 23], the variance of SCRs (VarSCR) [23], the mean amplitude (MAmp – mean value of the increases in SC between SCR initiations and SCR peaks) [7, 27], the maximum phasic amplitude (MaxPhAmp) [23], the amplitude sum of SCRs (AmpSum) [23], the magnitude [14, 17], the peak amplitude sum (PAmpSum) [19], the peak energy sum (PEngSum) [19], the sum of magnitudes [9, 10, 25], the first absolute difference (FAD) [12, 13], MFD [7], the mean of positive derivative [26], the mean of absolute derivative [26], the proportion of positive samples in derivative [26], the area of orienting responses [14, 17, 23, 25], the sum of the estimated areas under the responses [9, 10], the latitude (Lat) [23], the rise rate average (MRT) [19, 27], the peak rise time sum (PRTSum) [19], the decay rate average [19], the percentage decay [19], the half-recovery sum (HalfRecSum) [19], the duration [14, 17], the mean rise duration [7], and the sum of durations [9, 10, 25]. Besides, number of the nonspecific response [23] is also used. These features are extracted either from hand GSR [7, 12, 23, 27] or both hand and foot GSRs [11, 14, 16, 17, 20, 25, 26].

The respiration rate as well as the breathing amplitudes (BA) and the breathing durations vary between relaxed and stressed states. These metrics are analyzed on time-domain using the mean (MRESP) [9, 10, 14, 17, 20, 25], the standard error of the mean (SEM) [23], the median [20], the variance [9, 10, 20], and the standard deviation (SDRESP) [14, 17, 20, 25, 26] of the RESP signal; the respiration rate (RESPR) [7, 11, 15, 16, 23, 26], the ratio of heart rate or RESPR (HR/RESPR) [12], the central respiration frequency [23], the difference between maximal respiration and MRESP (range) [26]; the maximum breathing amplitude (MaxBA) [23], the minimum breathing amplitude (MinBA) [23], the mean of breathing amplitude (MBA) [7], the difference between

maximum and minimum values of breathing amplitude (MaxBA-MinBA) [23], the second difference of breathing amplitude (SDBA) [23], the MFD [7, 23], the mean of the second difference (MSD) [23], the standard deviation of the first difference (SDFD) [23], the standard deviation of the second difference (SDSD) [23]; the skewness [23], the kurtosis [23], and the entropy [13] measurements in the literature. In addition to time-domain measurements, these metrics are also analyzed in Fourier domain computing the spectral powers of RESP signals [10, 14, 17, 23, 25] within the bands 0-to-0.1 Hz, 0.1-to-0.2 Hz, 0.2-to-0.3 Hz, and 0.3-to-0.4 Hz.

Characteristics of increasing muscle activity in a stressed state are defined, in the literature, by the mean (MEMG) [9-11, 14, 16, 17, 20, 21], the variance [9, 20], the standard deviation [11, 20], the median [20], the zero-crossing-rate (ZCR) [21], the root-mean-square (RMS) [16, 21, 26], the root-mean-quad (RMQ) [28], the number of contractions per minute [11], the power spectrum [21], and the amplitude modulation of the envelope [21] measurements of the EMG signal.

III. EXPERIMENTAL STUDY

A. Database

The MIT-BIH PhysioNet Multi-parameter Database [29] is used for drivers' stress level recognition in this paper. This database consists of ECG, EMG, foot GSR, hand GSR, heart rate (HR), and respiration signals collected by Healey and Piccard [10] from wearable sensors on 17 automobile drivers while driving from MIT's East Garage to River Street Bridge and back through three cities and two highways between an initial rest and a final rest states. A marker in the database indicates the durations of rest states, city drive and highway drive. It is defined as one in rest state has low stress (LS) while he has moderate stress (MS) and high stress (HS) during highway and city drives, respectively in the database. The hand GSR, foot GSR, and respiration signals are sampled at 31 Hz while ECG and EMG signals are sampled at 496 and 15.5 Hz, respectively [10].

10 of the 17 drivers' bio-signals are used in this paper because of missing signals and non-clear markers of other drivers'. The list of these 10 drivers is given in Table 1.

Table 1. List of bio-signals'-used drivers.

Record Names				
drive5	drive6	drive7	drive8	drive9
drive10	drive11	drive12	drive15	drive16

B. Feature Extraction

1) ECG Features: Initially, a pre-processing is realized on ECG signals for time-domain feature extraction in order to remove baseline wander and muscle noise by applying a bandpass filter with cut-off frequencies of 0.5 Hz and 4 Hz. The time-domain ECG features in the literature related to HR and HRV are driven by the R-peaks of the ECG signal. Hence, R-peak detection is realized on the pre-processed ECG signals using inverted second derivative method [30]. In addition to the time-domain feature extraction, frequency-domain feature extraction on ECG signals is also realized for analyzing the energy distributions. The ECG features extracted in this paper are given in Table 2.

2) GSR Features: A Butterworth bandpass filter with cut-off frequencies of 0.1 Hz and 1 Hz is applied to hand GSR and foot GSR signals to remove baseline wander in these signals. The GSR features extracted from both hand GSR and foot GSR in this paper are given in Table 3.

3) Respiration Features: A pre-processing operation is performed on respiration signals to remove baseline wander and body movements related noises as given in [23]. This operation is realized by concatenating a moving-average filter and a 10^{th} order low pass filter with a cut-off frequency of 1 Hz [23]. The respiration features extracted in this paper are given in Table 4.

4) EMG Features: A Butterworth low pass filter with a cut-off frequency of 500 Hz is applied to EMG signals for removing noises caused by sudden body movements. The EMG features extracted in this paper are given in Table 5.

Table 2. The ECG features extracted for drivers' stress analysis.

	Time-Domain ECG Features	**Frequency-Domain ECG Features**
Features Related to HR	• MHR • SDHR	-
Features Related to HRV	• MNN • SDNN • RMSSD of NN intervals (RMSSD_NN) • NN50 • pNN50 • NN20 • pNN20 • MRR • SDRR • RMSSD of RR intervals (RMSSD_RR)	• TP • power of ultra-low frequency (ULF) (≤ 0.003 Hz) • VLF (0.003 Hz – 0.04 Hz) • LF (0.04 Hz – 0.15 Hz) • HF (0.15 Hz – 0.4 Hz) • VHF (≥ 0.4 Hz) • LF/HF

Table 3. The GSR features extracted for drivers' stress analysis.

Time-Domain GSR Features	
• MAmp	• MFD of GSR (MFD_GSR)
• PAmpSum	• MSC
• AmpSum	• VarSC
• MaxPhAmp	• SDSC
• NSCR	• HalfRecSum
• RSCR	• mean half recovery (HalfRecMean)
• MSCR	• Lat
• VarSCR	• PRTSum
• MSCL	• MRT
• VarSCL	• PEngSum

Table 4. The respiration features extracted for drivers' stress analysis.

Time-Domain Respiration Features		Frequency-Domain Respiration Features
• MRESP	• MaxBA-MinBA	
• SDDRESP	• range	
• SEM	• MFD of RESP (MFD_RESP)	
• skewness	• SDFD	• RESP power (0–0.1)
• kurtosis	• MSD	• RESP power (0.1–0.2)
• entropy	• SDSD	• RESP power (0.2–0.3)
• RESPR	• MSD of BA (MSD_BA)	• RESP power (0.3–0.4)
• HR/RESPR	• SDSD of BA (SDSD_BA)	
• MaxBA		
• MinBA		
• MBA		

Table 5. The EMG features extracted for drivers' stress analysis.

Time-Domain EMG Features
• MEMG
• RMS
• RMQ
• ZCR

The 86-dimensional feature vector of each driver is constructed by concatenating the features given in Tables 2-5 as given in the following.

$$\text{Feature Vector} = \begin{bmatrix} \text{Time - Domain ECG Features} \\ \text{Frequency - Domain ECG Features} \\ \text{Time - Domain Hand GSR Features} \\ \text{Time - Domain Foot GSR Features} \\ \text{Time - Domain RESP Features} \\ \text{Frequency - Domain RESP Features} \\ \text{Time - Domain EMG Features} \end{bmatrix} \tag{1}$$

C. Correlation Analysis

Pearson's correlation analysis of the extracted features with each other and with the stress levels is made. The Pearson's correlation r_{XY} between the n - dimensional signals X and Y is computed as:

$$r_{XY} = \frac{\sum_{i=1}^{n}(X_i - \bar{x})\cdot(Y_i - \bar{y})}{\sqrt{\sum_{i=1}^{n}(X_i - \bar{x})^2 \cdot \sum_{i=1}^{n}(Y_i - \bar{y})^2}} \tag{2}$$

where $\bar{x}$ and $\bar{y}$ are the means of X and Y, and X_i and Y_i are the i^{th} samples of X and Y, respectively. The correlation coefficient has a value in the $[-1,1]$ interval. Full correlation ($r_{XY} = 1$) shows that the signals X and Y are identical while negative full correlation ($r_{XY} = -1$) indicates that there is a 180^o phase shift between identical signals X and Y, and zero correlation ($r_{XY} = 0$) means that X and Y are completely

different signals. Strength of correlation between the features and between each feature and each stress level are analyzed based on the range given by [16] and shown in Table 6.

Table 6. Interpretation of the strength of correlation results [16].

Correlation Coefficient Range	Strength of Correlation
|0.00 -0.30|	Weak
|0.31 -0.50|	Moderate
|0.51 -0.80|	Strong
|0.81 -1.00|	Very strong

IV. RESULTS AND DISCUSSION

Pearson's correlation analysis of the features given in (1) with each other and with the stress levels is realized in this paper. A-dimension-reduced feature set for stress level recognition is constructed by concatenating the very strongly features of each stress level. Table 7 shows the features to be found as very strongly correlated with the low stress level. The absolute correlation values of these features with each other as well as with all stress levels are given in this table.

It is seen that the SDHR and the NN50 of ECG signals are full correlated. Hence, it is not necessary to use both of them for classification. Since the SDHR is more correlated with low stress level, the NN50 is eliminated from the feature set. Besides, the NSCR in hand GSR signals and the RESP powers between 0.1 Hz – 0.2 Hz and 0.2 Hz – 0.3 Hz are also full correlated with each other. On the score of stronger correlation of the RESP power between 0.2 Hz and 0.3 Hz with low stress level, it is kept in the feature set. Although the RESP power between 0.3 Hz – 0.4 Hz and the RMS of the EMG signals are not full correlated with any of the other features, they are very strongly and strongly correlated with the SDHR, respectively and not much correlated as the SDHR does with the low stress level. Hence, they are also excluded from the feature set.

Table 7. Correlation matrix obtained for features found to be very strongly correlated with the low stress level, including all stress levels.

	SDHR	NN50	NSCR (Hand)	RESP power (0.1–0.2)	RESP power (0.2–0.3)	RESP power (0.3–0.4)	RMS	LS	MS	HS
SDHR	1,000	1,000	0,194	0,208	0,195	0,998	0,782	0,924	0,164	0,536
NN50	1,000	1,000	0,194	0,208	0,195	0,998	0,782	0,918	0,140	0,534
NSCR (Hand)	0,194	0,194	1,000	1,000	1,000	0,239	0,722	0,851	0,643	0,689
RESP power (0.1–0.2)	0,208	0,208	1,000	1,000	1,000	0,254	0,733	0,872	0,704	0,147
RESP power (0.2–0.3)	0,195	0,195	1,000	1,000	1,000	0,240	0,723	0,886	0,623	0,185
RESP power (0.3–0.4)	0,998	0,998	0,239	0,254	0,240	1,000	0,813	0,880	0,433	0,241
RMS	0,782	0,782	0,722	0,733	0,723	0,813	1,000	0,887	0,548	0,774
LS	0,924	0,918	0,851	0,872	0,886	0,880	0,887	1,000	0.412	0.416
MS	0,164	0,140	0,643	0,704	0,623	0,433	0,548	0.412	1,000	0.592
HS	0,536	0,534	0,689	0,147	0,185	0,241	0,774	0.416	0.592	1,000

The features to be detected as very strongly correlated with the moderate stress level and their corresponding $|r_{XY}|$ values including all stress levels are given in Table 8. The TP of the ECG signals is included in the feature set since it is full correlated with the moderate stress level. Resulting from the high correlation of the ULF and the TP features of ECG signals and lower correlation of the ULF with moderate stress level, the ULF is removed from the feature set. The VarSCR within and the HalfRecSum of the hand GSR and the MaxPhAmp of the foot GSR signals are full correlated and they are also very strongly correlated with the LF

of the ECG signals and the MFD of the foot GSR signals. Among these features, due to the highest correlation with moderate stress level, only the MaxPhAmp of the foot GSR signals is remained in the feature set.

Table 8. Correlation matrix obtained for features found to be very strongly correlated with the moderate stress level, including all stress levels.

	TP	**ULF**	**LF**	**VarSCR**	**HalfRecSum (Hand)**	**MaxPhAmp (Foot)**	**MFD_GSR (Foot)**	**LS**	**MS**	**HS**
TP	1,000	0,955	0,696	0,230	0,244	0,231	0,203	0,137	1,000	0,118
ULF	0,955	1,000	0,843	0,452	0,466	0,454	0,426	0,087	0,937	0,062
LF	0,696	0,843	1,000	0,851	0,859	0,851	0,834	0,320	0,876	0,113
VarSCR	0,230	0,452	0,851	1,000	1,000	1,000	0,999	0,785	0,842	0,793
HalfRecSum (Hand)	0,244	0,466	0,859	1,000	1,000	1,000	0,999	0,568	0,806	0,298
MaxPhAmp (Foot)	0,231	0,454	0,851	1,000	1,000	1,000	0,999	0,152	0,885	0,637
MFD_GSR (Foot)	0,203	0,426	0,834	0,999	0,999	0,999	1,000	0,537	0,829	0,735
LS	0,137	0,087	0,320	0,785	0,568	0,152	0,537	1,000	0.412	0.416
MS	1,000	0,937	0,876	0,842	0,806	0,885	0,829	0.412	1,000	0.592
HS	0,118	0,062	0,113	0,793	0,298	0,637	0,735	0.416	0.592	1,000

The in between absolute correlation values of very strongly correlated features with the high stress level are indicated in Table 9, and the absolute correlation values of these features are given in Table 10. None of the features are full correlated but there exist very strongly correlated features. The MSCR in the hand GSR signals is highly correlated with the MinBA and the SDFD of the respiration signals. It is visible to use just the SDFD of respiration signals through these features since it is almost full correlated with the moderate stress level. In addition, the MFD and the HalfRecMean of the hand GSR signals are highly correlated and the HalfRecMean of the hand GSR signals is excluded from the feature set since the MFD of the hand GSR signals has a stronger correlation with this level of stress. Moreover, because the SDSD of the respiration signals is more correlated with the moderate stress level than the MaxBA-MinBA of which it is highly correlated, the MaxBA-MinBA is excluded from the feature set. Among these features in the feature set, all the features except the SDFD and the SDSD of the respiration signals due to their weaker correlations with high stress level are removed from the set.

Table 9. Correlation matrix obtained for features found to be very strongly correlated with the high stress level.

	AmpSum (Hand)	MSCR (Hand)	MFD_GSR (Hand)	HalfRecMean (Hand)	PEngSum (Hand)	MRT (Foot)	MBA	MaxBA - MinBA	SDFD	SDSD	SDSD_BA
AmpSum (Hand)	1,000	0,026	0,218	0,224	0,223	0,331	0,155	0,319	0,147	0,015	0,011
MSCR (Hand)	0,026	1,000	0,587	0,405	0,519	0,377	0,895	0,614	0,822	0,504	0,177
MFD_GSR (Hand)	0,218	0,587	1,000	0,907	0,655	0,359	0,530	0,261	0,477	0,292	0,028
HalfRecMean (Hand)	0,224	0,405	0,907	1,000	0,801	0,506	0,291	0,111	0,260	0,186	0,037
PEngSum (Hand)	0,223	0,519	0,655	0,801	1,000	0,733	0,315	0,113	0,380	0,197	0,316
MRT (Foot)	0,331	0,377	0,359	0,506	0,733	1,000	0,313	0,263	0,511	0,352	0,562
MBA	0,155	0,895	0,530	0,291	0,315	0,313	1,000	0,518	0,859	0,472	0,069
MaxBA - MinBA	0,319	0,614	0,261	0,111	0,113	0,263	0,518	1,000	0,754	0,920	0,611
SDFD	0,147	0,822	0,477	0,260	0,380	0,511	0,859	0,754	1,000	0,772	0,560
SDSD	0,015	0,504	0,292	0,186	0,197	0,352	0,472	0,920	0,772	1,000	0,725
SDSD_BA	0,011	0,177	0,028	0,037	0,316	0,562	0,069	0,611	0,560	0,725	1,000

Table 10. Correlation matrix of features, found to be very strongly correlated with the high stress level, with all stress levels.

	LS	MS	HS
AmpSum (Hand)	0,748	0,785	0,915
MSCR (Hand)	0,672	0,725	0,844
MFD_GSR (Hand)	0,609	0,780	0,962
HalfRecMean (Hand)	0,029	0,758	0,948
PEngSum (Hand)	0,365	0,699	0,939
MRT (Foot)	0,620	0,628	0,877
MBA	0,336	0,500	0,975
MaxBA-MinBA	0,197	0,348	0,969
SDFD	0,027	0,654	0,991
SDSD	0,577	0,224	0,984
SDSD_BA	0,045	0,599	0,975
LS	1,000	0.412	0.416
MS	0.412	1,000	0.592
HS	0.416	0.592	1,000

The resultant 6-dimensional feature set constructed by selecting almost uncorrelated features that are very strongly correlated with each of the stress levels, are given in Table 11.

Table 11. Selected features by correlation analysis.

Related Signal	Feature	Shows Very Strongly Correlation with
SDHR	ECG	Low stress
RESP power (0.2–0.3)	RESP	Low stress
TP	ECG	Moderate stress
MaxPhAmp	Foot GSR	Moderate stress
SDFD	RESP	High stress
SDSD	RESP	High stress

The stress level discriminating power of the selected features, given in Table 10, is measured by the Accuracy (ACC) and the False Positive Rate (FPR) metrics succeeded by the kNN (k=5), random forest, decision tree, LLC, and SVM classifiers. The classification procedure is realized by 5-fold cross-validation technique. These metrics are computed by using the following relations,

$$\%\,\mathrm{ACC} = \frac{\mathrm{TP}+\mathrm{TN}}{\mathrm{TP}+\mathrm{TN}+\mathrm{FP}+\mathrm{FN}}\cdot 100 \tag{3}$$

$$\%\,\mathrm{FPR} = \frac{\mathrm{FP}}{\mathrm{FP}+\mathrm{TN}}\cdot 100 \tag{4}$$

where TP, TN, FP, and FN refer to the numbers of true positives, true negatives, false positives, and false negatives, respectively. These metrics are computed for each of the five folds, and the mean and the standard deviations of the computations are evaluated. The same classification process is also executed by the full feature set given in (1) for comparison. The classification results of both full and selected feature sets are shown in Figure 1. An average increment of 24.85% in mean ACC and an average decrement of 88.01% in mean FPR are satisfied by using the selected feature set for drivers' stress level recognition. Besides the classification success, the decrement in standard deviations of the performance metrics indicates the data independency of the selected feature set.

Although an overall classification accuracy of 100% is achieved by most of the classifiers using the selected feature set, the SVM and the LLC classifiers succeeded an accuracy of 95.56% and a FPR of 3.33%.

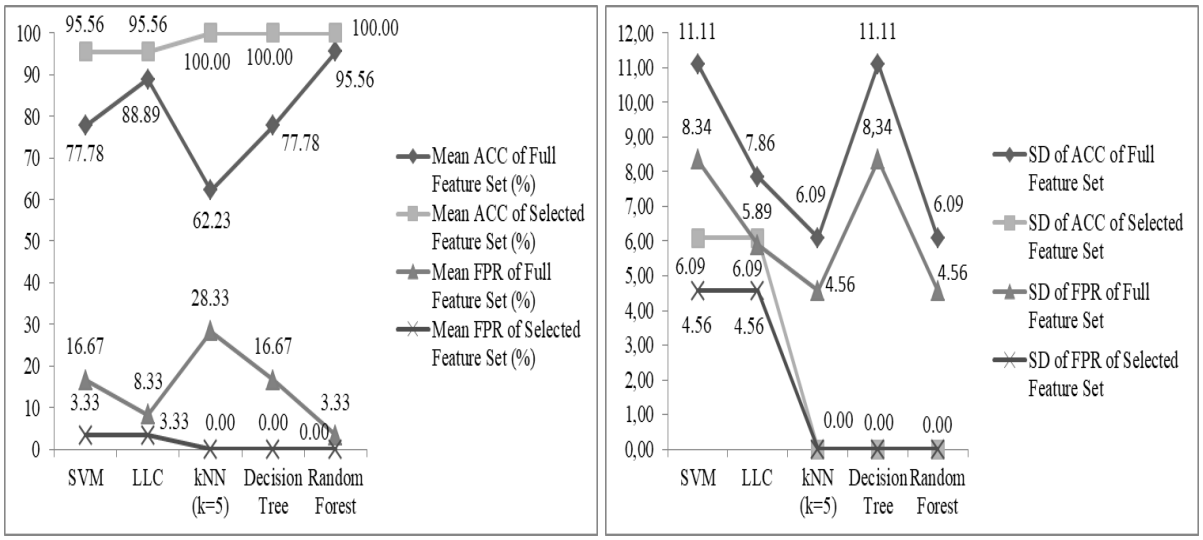

Figure 1. Classification results of drivers' stress level recognition

Analyzing the total confusion matrices of these classifiers given in Table 12, it is seen that although high stress level is perfectly detected, the non-100% accuracies are because of the inter-belonged FPs and FNs of

low and moderate stress levels. These misclassifications are thought to be caused by the closeness of correlation strength of the RESP power (0.2–0.3) with low and moderate stress levels.

Table 12. The total confusion matrices achieved by classifying the selected feature set via SVM and LLC classifiers.

		Classified Stress Levels by					
		SVM Classifier			LLC Classifier		
		Low Stress	Moderate Stress	High Stress	Low Stress	Moderate Stress	High Stress
Actual Stress Levels	Low Stress	9	1	0	9	1	0
	Moderate Stress	1	9	0	1	9	0
	High Stress	0	0	10	0	0	10

In conclusion, low, moderate, and high stress levels are recognized by 93.33%, 93.33%, and 100% accuracies, respectively.

V. CONCLUSIONS

A correlation analysis of frequently used physiological measurements, computed from the ECG, hand GSR, foot GSR, RESP, and EMG signals for drivers' stress level recognition, is realized in this paper. The experimental study is executed on the publicly available MIT-BIH PhysioNet Multi-parameter Database [10]. The correlation analysis is concluded in proposal of almost uncorrelated feature pairs for each stress level with very strong intra-level and relatively weak inter-level correlations. These feature pairs indicate that the SDHR and the RESP power within the band 0.2-0.3 Hz shows a significant difference in low stress level while the TP of the ECG signal and the MaxPhAmp of the foot GSR have high significance for moderate stress level and SDFD and SDSD are discriminators for high stress level. The strength of these features are verified by a classification procedure using kNN (k=5), random forest, decision tree, LLC, and SVM classifiers with by 5-fold cross-validation technique. The recognition ACC is raised up to 100% with an average increment of 24.85%, and the FPR is decreased up to 0% by providing a reduction rate of 88.01% on average when the proposed feature set is used instead of the full feature set. Besides, the proposed feature set satisfies these results in less time consumption which is extremely important for real-time applications. In addition, the data independency of these features is approved by the reduced and mostly zeroed standard deviations of both ACC and FPR. These outcomes clearly show that the proposed feature set can confidently be integrated into the driving assistance systems in new generation vehicles.

REFERENCES

[1] Selye, H. (1976). *Stress without distress*. *Psychopathology of Human Adaptation Serban G. (Eds.)*. Springer, Boston, MA, 137-146.

[2] Rastgoo, M. N., Nakisa, B., Rakotonirainy, A., Chandran, V., & Tjondronegoro, D. (2018). A critical review of proactive detection of driver stress levels based on multimodal measurements. *ACM Computing Surveys*, 51, 1–35.

[3] Beirness, D. J. (1993). Do we really drive as we live? The role of personality factors in road crashes. *Alcohol, Drugs, and Driving: Abstracts and Reviews*, 9 (3), 129-143. ·

[4] Simon, F. & Corbett, C. (1996) Road traffic offending, stress, age, and accident history among male and female drivers. *Ergonomics*, 39 (5), 757–780.

[5] Miller, L. H., Smith, A. D., & Rothstein, L. (1994). *The Stress Solution: An Action Plan to Manage the Stress in Your Life reprint ed.*, Pocket Books, New York.

[6] Rodrigues, J. G. P., Kaiseler, M., Aguiar, A., Cunha, J. P. S., & Barros, J. (2015). A mobile sensing approach to stress detection and memory activation for public bus drivers. *IEEE Transactions on Intelligent Transportation Systems*, 16, 3294–3303.

[7] Katsis, C. D., Katertsidis, N., Ganiatsas, G., & Fotiadis, D. I. (2008). Toward emotion recognition in car-racing drivers: A biosignal processing approach, *IEEE Transactions on Systems, Man, and Cybernetics - Part A*. 38 (3), 502–512.

[8] Rigas, G., Katsis, C. D., Bougia, P., & Fotiadis, D. I. (2008). A Reasoning-Based Framework for Car Driver's Stress Prediction. *16. Mediterranean Conference on Control and Automation*, 25-27 June, Ajaccio, France, 627–632.

[9] Healey, J. & Picard, R. (2002). SmartCar: Detecting Driver Stress. *15. International Conference on Pattern Recognition*, 3-7 September, Barcelona, Spain, 4, 218–221.

[10] Healey, J. A. & Picard, R. W. (2005). Detecting stress during real-world driving tasks using physiological sensors, *IEEE Transactions on Intelligent Transportation Systems*, 6 (2), 156–166.

[11] Akbaş, A. (2011). Evaluation of the physiological data indicating the dynamic stress level of drivers, *Scientific Research and Essays*, 6 (2), 430-439.

[12] Rigas, G., Goletsis, Y., Bougias, P., & Fotiadis, D. I. (2011). Towards driver's state recognition on real driving conditions. *International Journal of Vehicular Technology*, 2011, 1-14.

[13] Rigas, G., Goletsis, Y., & Fotiadis, D. (2012). Real-time driver's stress event detection. *IEEE Transactions on Intelligent Transportation Systems*, 13 (1), 221–234.

[14] Deng, Y., Wu, Z., Chu, C. H., & Yang, T. (2012). Evaluating Feature Selection for Stress Identification. *IEEE 13. International Conference on Information Reuse & Integration*, 8-10 August, Las Vegas, NV, USA, 584–591.

[15] Soman, K., Alex, V., & Srinivas, C. (2013). Analysis of Physiological Signals in Response to Stress using ECG and Respiratory Signals of Automobile Drivers. *2013 International Mutli-Conference on Automation, Computing, Communication, Control and Compressed*, 22-23 March, Kottayam, Kerala, India, 574-579.

[16] Singh, M. & Bin Queyam, A. (2013). A novel method of stress detection using physiological measurements of automobile drivers. *International Journal of Electronics Engineering*, 5 (2), 13–20.

[17] Deng, Y., Wu, Z., Chu, C. H., Zhang, Q., & Hsu, D. F. (2013). Sensor feature selection and combination for stress identification using combinatorial fusion. *International Journal of Advanced Robotic Systems*, 10, 306-313.

[18] Wang, J. S., Lin, C. W., & Yang, Y. T. C. (2013). A k-nearest-neighbor classifier with heart rate variability feature-based transformation algorithm for driving stress recognition. *Neurocomputing*. 116, 136–143.

[19] Singh, R. R., Conjeti, S., & Banerjee, R. (2013). A comparative evaluation of neural network classifiers for stress level analysis of automotive drivers using physiological signals, *Biomedical Signal Processing and Control*, 8 (6), 740-754.

[20] Avcı C., Akbaş, A., & Yüksel, Y. (2014). Evaluation of Statistical Metrics by using Physiological Data to Identify the Stress Level of Drivers. *3. International Conference on Environment, Chemistry and Biology*, 29-30 November, Port Louis, Mauritius, 124-128.

[21] Soman, K., Sathiya, A., & Suganthi, N. (2015). Classification of Stress of Automobile Drivers using Radial Basis Function Kernel Support Vector Machine. *2014 IEEE International Conference on Information Communication & Embedded Systems*, 27-28 February, Chennai, India, 1-5.

[22] Keshan, N., Parimi, P.V., & Bichindaritz, I. (2015). Machine Learning for Stress Detection from ECG Signals in Automobile Drivers. *2015 IEEE International Conference on Big Data*, 29 October-1 November, Santa Clara, CA, USA, 2661–2669.

[23] Lanatà, A., Valenza, G., Greco, A., Gentili, C., Bartolozzi, R, Bucchi, F., Frendo, F, & Scilingo, E. P. (2015). How the autonomic nervous system and driving style change with incremental stressing conditions during simulated driving. *IEEE Transactions on Intelligent Transportation Systems*, 16 (3), 1505-1517.

[24] Heikoop, D. D., de Winter, J. C. F., Arem, B, & Stanton, N. A. (2016). Effects of platooning on signal-detection performance, workload, and stress: A driving simulator study. *Applied Ergonomics*, 60, 116-127.

[25] Chen, L., Zhao, Y., Ye, P., Zhang, J., & Zou, J. (2017). Detecting driving stress in physiological signals based on multimodal feature analysis and kernel classifiers. *Expert System with Applications*, 85, 279-291.

[26] Ollander, S., Godin, C., Charbonnier, S., & Campagne, A. (2016). Feature and Sensor Selection for Detection of Driver Stress. *3. International Conference on Physiological Computing Systems*, 27-28 July, Lisbon, Portugal, 115–122.

[27] Urbano, M., Alam, M., Ferreira, J., Fonseca , J., & Simíões, P. (2017). Cooperative Driver Stress Sensing İntegration with Ecall System for Improved Road Safety. *17. International Conference on Smart Technologies*, 6-8 July, Ohrid, Macedonia, 883-888.

[28] Zheng, R., Yamabe, S., Nakano, K., & Suda, Y. (2015). Biosignal analysis to assess mental stress in automatic driving of trucks: palmar perspiration and masseter electromyography. *Sensors*, 15, 5136-5150.

[29] Goldberger A. L., Amaral L. A. N., Glass L., Hausdorff J. M., Ivanov P. Ch., Mark R. G., Mietus J. E., Moody G. B., Peng C-K., & Stanley H. E. (2000). PhysioBank, PhysioToolkit, and PhysioNet: components of a new research resource for complex physiologic signals. *Circulation*, 101 (23), 215-220.

[30] Deshmukh, S. V. (2018). Study of online driver distraction analysis using ECG-dynamics. Master of Science Thesis, University of Michigan, Computer and Information Sciences, Dearborn, Michigan.